AD-A094 558   MASSACHUSETTS INST OF TECH CAMBRIDGE   F/G 20/5
A MULTILEVEL MODEL OF XEF GROUND STATE KINETICS,(U)
1977   S F FULGHUM, M S FELD, A JAVAN   N00014-76-C-0447
UNCLASSIFIED   NL

1 OF 1
AD
A094 558

END
DATE
FILMED
2-81
DTIC

1 of 24

LEVEL II

(1)

(6) A Multilevel Model of XeF Ground State Kinetics*

(10) S.F. Fulghum[†], M.S. Feld, ~~and~~ A. Javan

(12) 24

(11) 1977

ABSTRACT

We present a multilevel model of energy transfer ^is in the XeF ground electronic state due to collision-induced VT and dissociation processes. The model, whose parameters are based on experimental results presented here and on other recent data, should be useful in accurate simulations of output efficiency and multiline laser oscillation in XeF. Effective lifetimes of individual ground state levels, applicable to two level laser models, are determined from the multilevel model. The effective lifetime of the primary lower laser level, v"=3, is determined to be 4 to 6 nsec for a 1 atm He buffer.

(15) N00014-76-C-0447

---

[*] Work supported by NSF and in part by the Office of Naval Research

[†] Currently with Avco Everett Research Laboratory, Inc.

Introduction

In the early 1960's xenon was found to form stable compounds with fluorine, such as XeF_2, XeF_4, and XeF_6. The monohalide, XeF, however, was never isolated and was assumed to have a repulsive ground state. The emergence of rare gas monohalides as UV laser candidates in 1974 (1) again focused attention on XeF. The vibrational and rotational structure observed in laser fluorescence made it obvious that the transitions were bound-bound. This structure was analyzed by Tellinghuisen and co-workers, who determined that the ground state is indeed bound by about 1200 cm^{-1}, that it is highly anharmonic, and that it supports about 10 vibrational levels (Fig. 1).(2,3) The molecule is not stable in a practical sense because the shallow potential well allows rapid dissociation by collisional processes.

The efficiency of an XeF laser is limited by the rate at which these collisions with a buffer gas remove molecules from the relatively high lying levels on which the laser transitions terminate ($v''=2,3,4$). Population can be removed from these levels through collision-induced vibrational transitions (VT), collision-induced dissociation and by rotational equilibration, which can carry molecules to unstable rotational levels above the centrifugal barrier. Our aim has been to measure these rates directly and to estimate their effects on XeF laser behavior. We will report our most recent measurements of the overall dissociation rate of XeF in a He buffer and the results of a model designed to extract VT and dissociation rates from the data. Such a multilevel model of the XeF ground state should be useful in laser simulations where accurate and detailed results are required.

Experimental Method

The method used is the technique reported previously in which XeF^* is produced by the photodissociation of XeF_2 with a 20 nsec ArF laser pulse.(4) This XeF^* rapidly decays via spontaneous emission, creating an initial nonequilibrium population distribution in the electronic ground state, primarily in levels $v''= 2,3$ and 4, since transitions terminating on these levels have the largest Franck-Condon factors.(3) After a measured delay, a 20 nsec pulse from a tunable UV dye laser, tuned to an appropriate B-X vibronic transition, probes a specific lower vibrational level. The fluorescence induced by the dye laser is proportional to the population in the level at that time. The rise of population in say $v''=0$, as population flows down from $v''=2$, 3 and 4, is a measure of the VT rates in XeF. The subsequent decay of this population, after a quasiequilibrium is established, is determined by both the VT rates and the direct dissociation rates out of individual levels. Figure 2 shows the buildup and decay of population in v"=0 at various pressures of a He buffer. The tail of each set of points is well described by an exponential decay. Figure 3 plots these exponential decay rates versus pressure, along with a linear fit which gives the overall decay rate of a system in a quasiequilibrium.(4)

VT and Dissociation Rate Models

These experiments measure the net buildup and decay rates of population in a given level in the ground state. The problem is to extract from these measurements values for specific rates, such as the VT rate from v"=3 to v"=2 or the direct dissociation rate out of v"=3. Obviously, there are a great many such rates and to determine them individually from a few such measurements is not possible. The approach taken is to fit the experimental data with a model which expresses all of these rates with only a few parameters.

The overall model consists of two parts. One part describes the VT and dissociation rates of an XeF-buffer system and uses four parameters. These are the quantities required to estimate the effects of ground state kinetics on a laser system. The second part of the model describes effects particular to this experiment (and absent in a laser plasma) such as the background dissociation due to the XeF_2. The XeF-buffer system will be treated first.

The information theoretic approach of Procaccia and Levine is particularly well suited to expressing the VT rates in a convenient form.(5) It provides a set of "prior" VT rates using a single rate parameter and the known energy levels of the XeF molecule. Actual rates are then related to these prior rates in terms of the "surprisal", a measure of deviation. This surprisal parameter follows the well-known "exponential gap rule" which generally indicates that VT transitions involving large changes in vibrational energy have a lower probability of occurrence. Thus only two parameters need to be determined by the experiments to determine all of the VT rates. The specific form of the VT rate from v"=i to v"=j, k_{ji}, is taken to be:(5,6,7)

$$k_{ji} = C_v \left[\frac{e^{\Delta} \Delta^2 K_2(\Delta)}{B_j} \right] e^{-2\lambda|\Delta|} , \qquad (1)$$

$$\Delta = (E_j - E_i)/2 ,$$

where E_i is the energy of the ith level, $K_2(\Delta)$ is the modified Bessel function of the second kind of order 2, B_j is the rotational constant of the final state and C_v and λ are the constants to be determined.

The overall dissociation of XeF is determined by these VT rates and by the direct dissociation rate out of each individual level. A variation of the Arrhenius equation is used to model these dissociation rates. It includes an overall rate parameter and a vibrational bias parameter which allows for a dependence of the dissociation rate on the actual level of vibrational excitation. The form of the direct, collision-induced dissociation rate out of level v"=i, d_i, is thus taken to be:(8)

$$d_i = C_D \, e^{\frac{\beta E_i}{D_0}} \, e^{-(D_0 - E_i)/kT} \quad , \qquad (2)$$

where E_i is the energy of the vibrational level at the peak of its rotational manifold (J=24), D_0 is the peak of the centrifugal barrier for J=24 and C_D and β are the constants to be determined.

The following set of equations uses the above rates to describe the relaxation of the vibrational level populations, N_i, in an XeF-buffer system.

$$\dot{N}_i = -d_i N_i + \sum_{j \neq i} \left(k_{ij} N_j - k_{ji} N_i \right) \qquad (3)$$

Note that once the rate constants are determined by a room temperature experiment, Eqs. (1) and (2) allow extrapolation to higher temperatures.

To limit the number of parameters to be varied in the fits we have fixed λ and C_D. Rubinson and Steinfeld have analyzed their extensive data on inelastic collisions of I_2^*

with rare gas atoms and find that this data is well described by the surprisal model with λ in the range of 2.5 to 4.5.(6) An early calculation by Huestis used the data of Refs. 6 and 9 and the exponential gap representation with $\lambda \cong 3$ to estimate the role of VT rates and collisional dissociation on XeF laser behavior.(10) Theoretical calculations by Duzy and Shui, which use a combination of phase-space theory and semi-classical trajectory calculations, indicate that λ for XeF and a Ne buffer is between 2 and 3.(11) We choose $\lambda = 3$ for our analysis.

For a given β the overall dissociation rate parameter C_D can be fixed by assuming that molecules in vibrational states at the dissociation limit will dissociate at the gas kinetic rate, which is taken to be 3×10^{-10} cm^3 sec^{-1}. In addition, since the peak of the rotational manifold (J=24) in levels $v''=8$ and 9 is above the centrifugal barrier, these levels are presumed to dissociate at the gas kinetic rate and reverse processes from these levels are set equal to zero.

As mentioned previously, in fitting our data two additional parameters are introduced to describe the effects of XeF_2. (These parameters are not used for laser modeling.) Even though we work at relatively low pressures of XeF_2 compared to He, XeF_2 is still effective in dissociating XeF. This effect can be seen in Fig. 3, which shows a background rate, primarily due to the XeF_2. In the experimental fits this background rate is modeled by a single overall exponential decay. The fits to the v"=0 data (Fig. 2) use a background rate of $4.5x10^5$ sec^{-1}. The v"=1 data reported previously (4) (Fig. 4) show a somewhat lower background rate and are fit with a $2.5x10^5$ sec^{-1} overall rate.

Another effect due to the XeF_2 is a mixing of the two lowest vibrational levels. Figure 4 shows the buildup and decay of population in v"=1 at 5 and 20 Torr of He. Although the v"=1 data rises somewhat faster than that of v"=0, Eq. (3) predicts an even faster rise rate and a sharper peak for v"=1. This suggests that, in the experiment, the two levels are closely coupled, possibly by the near resonance between the ν_2 bending mode of XeF_2 (212 cm^{-1})(12) and the 0-1 vibrational transition of XeF (204 ± 4 cm^{-1}).(3) To simulate this effect a mixing rate of $1.5x10^6$ sec^{-1} is included in the model between levels 0 and 1, which is approximately the gas kinetic rate for collisions between XeF and XeF_2.

To establish that the background rate is, in fact, primarily due to XeF_2, additional data was taken at a reduced XeF_2 pressure. By lowering the temperature of the cold finger containing the solid XeF_2 from 0 °C to -18 °C, the vapor pressure was reduced by a factor of 6 to 0.1 Torr. Figure 5 shows data for v"=0 with 10 Torr of He. The solid curve is the result of the model using the parameters from the 0°C fit (described below) except that the background rate and the 0-1 mixing rate are reduced by a factor of 6. Although the data is noisy, it clearly indicates that the XeF_2 is the primary cause of the background dissociation.

Fit to Experimental Data

These rates are incorporated into a 10-level model of the ground state (Eq. 3 with XeF_2 terms added), which can be solved using numerical matrix methods. The initial population is assumed to be equally distributed among levels v"=2,3 and 4 since the Franck-Condon factors into these levels dominate and are roughly equal (3) . The results are not very sensitive to the particular distribution assumed among these higher levels. The negative eigenvalue of the rate matrix with the smallest absolute value is the overall decay rate of the system in a quasiequilibrium. This overall decay has been measured both by two exponential fits (4) to the new data (Fig. 3) and by previous absorption experiments. (13) The minimum eigenvalue is typically about ten times smaller than the next, giving an unambiguous overall decay rate. The positive exponentials, however, are typically quite close together, so that no individual rate can characterize the rising portion of the data. This model was fit to the data in Fig. 2 by adjusting the two free parameters until the peaks were matched as closely as possible, while maintaining a minimum eigenvalue close to the measured overall decay rate. The solid curves in Fig. 2 are plots of the final fit using the buffer gas pressure as the final parameter. The primary parameters used in the fit are:

$$C_V = 1.0\times10^{-12}\ \text{cm}^2\ \text{sec}^{-1} \qquad \lambda = 3$$
$$C_D = 6.1\times10^{-12}\ \text{cm}^3\ \text{sec}^{-1} \qquad \beta = 3.9 \qquad (4)$$

with the background rate set at 4.5×10^5 sec^{-1} and the 0-1 mixing rate at 1.5×10^6 sec^{-1}.

These results indicate that, with regard to the removal of population from levels $v''=2,3$ and 4, direct dissociation is as effective or more effective than vibrational relaxation. Direct dissociation can be faster than VT processes because it includes both vibrational and rotational energy transfer.

XeF laser behavior can be modeled by supplementing Eqs. (1)-(3) and the parameters of Eq. (4) with similar rate equations for at least two upper laser levels, laser pumping terms, source terms and equations for the output intensities. Such a model is essential for the accurate estimation of energy extraction efficiency, and for describing multilevel processes such as bottlenecking and competition between the three primary transitions, 0-2, 0-3 and 1-4 (Fig. 1).

Specific examples of laser modeling of this type can be found in Ref. 7.

Effective Lifetimes

The multilevel model described above may be unnecessarily complex for some applications. If only the primary transition, 0-3, needs to be modeled, a two level model may give fairly accurate results. In this limit the ground state vibrational manifold is represented by a single level which decays with an effective lifetime, τ . This lifetime relates the steady state population, N_L° , in the lower level to the rate of supply of population, Λ , into that level, due to both stimulated and spontaneous emission:

$$N_L^\circ = \tau \Lambda . \tag{5}$$

In this case the effective lifetime is simply the inverse of the total dissociation rate out of the lower level. For the two level laser model such quantities as laser extraction efficiency and output power are proportional to

$$1 - \frac{\tau}{\tau_R} , \tag{6}$$

where τ_R is the radiative lifetime of the upper laser level.(7)

This simple effective lifetime can be related to the multilevel model and experimental parameters described above. In a multilevel system a rate into any one level results in population flowing into neighboring levels also, so that relating the steady state populations to the constant rates into each level requires a matrix. This effective lifetime matrix can be determined numerically, column by column, by introducing a unit source term into that particular vibrational level in Eq. (3). The resulting steady state populations are the elements of this lifetime matrix. We find that the diagonal elements dominate, which means that, to a good approximation, the simple definition of an effective lifetime is applicable to the higher levels such as v"=2,3 and 4. For equal rates into these three levels, the equilibrium populations predicted by the model using the parameters of Eq. (4) gives

$$\tau(4) = 1.5, \quad \tau(3) = 4.5, \quad \tau(2) = 12.2 \text{ nsec atm}, \tag{7}$$

where $\tau(v'')$ denotes the effective lifetime of the v" level. Since 0-3 is the primary lasing transition at room temperature, the value of $\tau(3)$ would be the effective lifetime most appropriate to use in a two level model of the XeF laser. Comparisons between two level laser models and laser models with a ten level ground state vibrational manifold show good agreement for laser efficiency if a 4 nsec effective lifetime is used in the two level case.(7) This indicates [Eq. (6)] that the finite lifetime of the lower laser levels decreases the laser extraction efficiency by about 30% at one atmosphere, in reasonable agreement with calculations based on the multilevel model. These lifetimes, in themselves, do not preclude steady state or long pulse lasing at one atmosphere.

Effect of Increased Temperature

There is considerable interest in the increased efficiency of XeF lasers run at elevated temperatures.(14) Our models of the VT rates and direct dissociation rates [Eqs. (1),(2)] can be used to extrapolate our room temperature measurements of these rates to elevated temperatures. At 450 °C, this gives:

$$\tau_{450}(4) = 0.5, \quad \tau_{450}(3) = 1.2, \quad \tau_{450}(2) = 2.6 \text{ nsec amagat.} \qquad (8)$$

Thus, raising the temperature to 450 °C should increase the extraction efficiency by about 20%, at least insofar as the effects of increased VT and dissociation rates are concerned. Since the observed increase in efficiency is about a factor of two(14), most of the increased efficiency should be due to other processes, such as a decrease in absorption at higher temperatures.(15) The multilevel model can be used for detailed predictions of the relative intensities of the laser emission at the primary transitions under these conditions.(7)

Error Estimate

Finally, the question of the probable error in these measurements and models must be addressed. The overall dissociation rate is fairly well defined now by the two different types of experiments we have performed.(4,13) The value of $9.9(\pm 2.5)\times 10^{3}$ sec^{-1} Torr^{-1} is not dependent on the details of the model we have chosen to represent the equilibration and dissociation of the ground state. The VT rate and dissociation rate parameters are not as well defined. This is due to the difficulty of fitting exponential curves of this form and the limited data that we have in the rising portion of the data sets.

In general, the model fits the data quite well at 10, 25 and 45 Torr of He, where the expected rise times are not too fast. The curve at 95 Torr, however, shows that either the experiment cannot properly measure rise times of less than about 300 nsec or that other kinetic processes not considered in the model occur which slow the rise rate immediately after the photodissocation of the XeF_2. The same effect is seen in the $v''=1$ data at 20 Torr, where the rise time is again predicted to be faster. This is possibly an effect of the

XeF_2 background.

A good way to indicate the practical effects of possible errors in the parameters is to show how they change the simple effective lifetimes. The assumption of a mixing rate between v"=0 and 1 increases the rise time of the v"=0 population in the model, which must be offset by a decrease in C_V to fit the peaks. Thus the C_V parameter determined by the fits could be low by a factor of two or possibly three. Using a C_V of 3×10^{-12} cm^2 sec^{-1} and decreasing the direct dissociation rates to maintain the same overall dissociation rate gives

$$\tau'(4) = 1.9, \qquad \tau'(3) = 6.1, \qquad \tau'(2) = 15.8 \text{ nsec atm,} \qquad (9)$$

which are reasonably close to the results of Eqs. (7). This is not surprising, since the effective lifetime of a level, neglecting the return flow of population from neighboring levels, is approximately

$$(\gamma_V + \gamma_D)^{-1} \qquad (10)$$

where γ_V is the total VT rate out of the level and γ_D is the direct dissociation rate out of the level.(7) Increasing one while decreasing the other tends to leave their sum unchanged.

The overall decay rate from the experimental fit (in the absence of XeF_2) is 8.25×10^3 sec^{-1} $Torr^{-1}$. Assuming a faster rate of 1×10^4 sec^{-1} $Torr^{-1}$ gives $\tau'(3)$= 3.9 nsec atm, while a slower rate of 6.5×10^3 sec^{-1} $Torr^{-1}$ gives $\tau'(3)$=5.4 nsec atm. Assuming λ=2 instead of 3 while maintaining a constant VT rate from v"=0 to 1 (to maintain the peak positions) only changes $\tau'(3)$ to 4.6 nsec atm. The effective lifetime of the primary lower laser level, v"=3, is thus within the range of 4 to 6 nsec atm.

Summary

In conclusion, we have developed a multilevel model of the XeF ground electronic state vibrational manifold which includes dissociation and vibrational equilibration rates. This model has been fit to experimental data to derive rate parameters which can be used for accurate estimates of XeF laser extraction efficiency and for modeling aspects of laser behavior involving more than one transition. Effective lifetimes for individual levels are derived which can be used in simpler two level laser models. The temperature dependence predicted by these models should prove useful in determining conditions under which laser efficiency is optimized.

REFERENCES

(1) J.E. Velazco and D.W. Setser, "Bound-free emission spectra of diatomic xenon halides," J. Chem. Phys., vol. 62, pp. 1990-1991, 1975

(2) J. Tellinghuisen, P.C. Tellinghuisen, G.C. Tisone, J.M. Hoffman, and H.K Hayes, "Spectroscopic studies of diatomic noble gas halides. III Analysis of XeF 3500 Å band system," J. Chem. Phys., vol. 68, pp. 5177-5186, 1978

(3) P.C. Tellinghuisen, J. Tellinghuisen, J.A. Coxon, J.E. Velazco, and D.W. Setser, "Spectroscopic studies of diatomic noble gas halides. IV Vibrational and rotational constants for the X,B and D states of XeF," J. Chem. Phys., vol. 68, pp. 5187-5198, 1978

(4) S.F. Fulghum, M.S. Feld, and A. Javan "XeF ground state dissociation and vibrational equilibration," Appl. Phys. Lett., vol. 35, pp. 247-249, 1979

(5) I. Procaccia and R.D. Levine, "Vibrational energy transfer in molecular collisions: An information theoretic analysis and synthesis," J. Chem. Phys., vol. 63, pp. 4261-4279, 1975

(6) M. Rubinson and J.I. Steinfeld, "Entropy analysis of product energy distributions in nonreactive inelastic collisions," Chem. Phys., vol. 4, pp. 467-475, 1974

(7) S.F. Fulghum, Ph.D. thesis, M.I.T., 1980 (unpublished)

(8) J.H. Kiefer, H.P.G. Joosten, and W.D. Breshears, "On the preference for vibrational energy in diatomic dissociation," Chem. Phys. Lett., vol. 30, pp. 424-428, 1975

(9) R.B. Kurzel and J.I. Steinfeld, "Energy-transfer processes in monochromatically excited iodine molecules. III Quenching and multiquantum transfer from v'=43," J. Chem. Phys., vol. 53, pp.3293-3303, 1970

(10) D.L. Huestis, R.M. Hill, D.J. Eckstrom, M.V. McCusker, D.C. Lorents, H.H. Nakano, B.E. Perry, J.A. Margevicius, and N.E. Schlotter, "New electronic transition laser systems," SRI International Technical Report No. MP 78-07, pp. 113-118, May 1978

(11) C. Duzy, private communication

(12) U. Nielsen and W.H.E. Schwarz, "VUV spectra of the xenon fluorides," Chem. Phys., vol. 13, pp. 195-202, 1976

(13) S.F. Fulghum, I.P. Herman, M.S. Feld, and A. Javan, "XeF ground-state dynamics in a laser discharge," Appl. Phys. Lett., vol. 33, pp. 926-928, 1978

(14) J.C. Hsia, J.A. Mangano, J.H. Jacob, and M. Rokni, "Improvement in XeF laser efficiency at elevated temperatures," Appl. Phys. Lett., vol. 34, pp. 208-210, 1979

(15) L.F. Champagne, "Temperature-dependent absorption processes in the XeF laser," Appl. Phys. Lett., vol. 35, pp. 516-519, 1979

FIGURES

Fig. 1. XeF B and X state vibrational levels and primary laser transitions.

Fig. 2. Net buildup and decay of population in $v''=0$ with a He buffer as indicated by induced fluorescence. XeF_2 at 0.6 Torr. Solid curve is the multilevel model fit.

Fig. 3. Decay rate of population in $v''=0$ from data in Fig. 1 (dots) compared to data published previously in Ref. 4 (crosses). Slope of linear fit is 9.9×10^3 sec^{-1} $Torr^{-1}$.

Fig. 4. Population in $v''=1$ with a He buffer and XeF_2 at 0.6 Torr. Solid curve is the multilevel model fit.

Fig. 5. Population in $v''=0$ with a He buffer and XeF_2 at 0.1 Torr. Solid curve is the multilevel model fit.

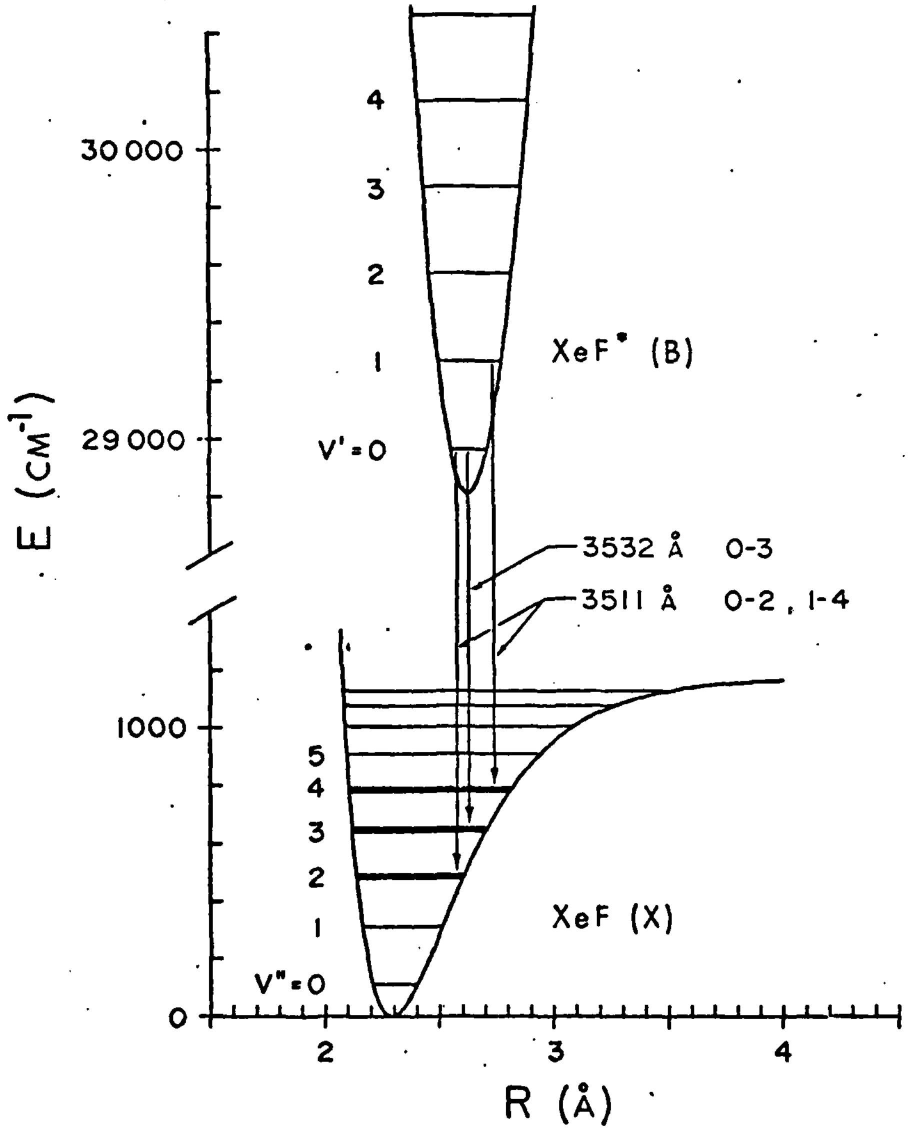
E (CM^{-1})
30 000
29 000
1000
0
4
3
2
1
V' = 0
XeF* (B)
3532 Å 0-3
3511 Å 0-2, 1-4
5
4
3
2
1
V" = 0
XeF (X)
2
3
4
R (Å)

FIGURE 1

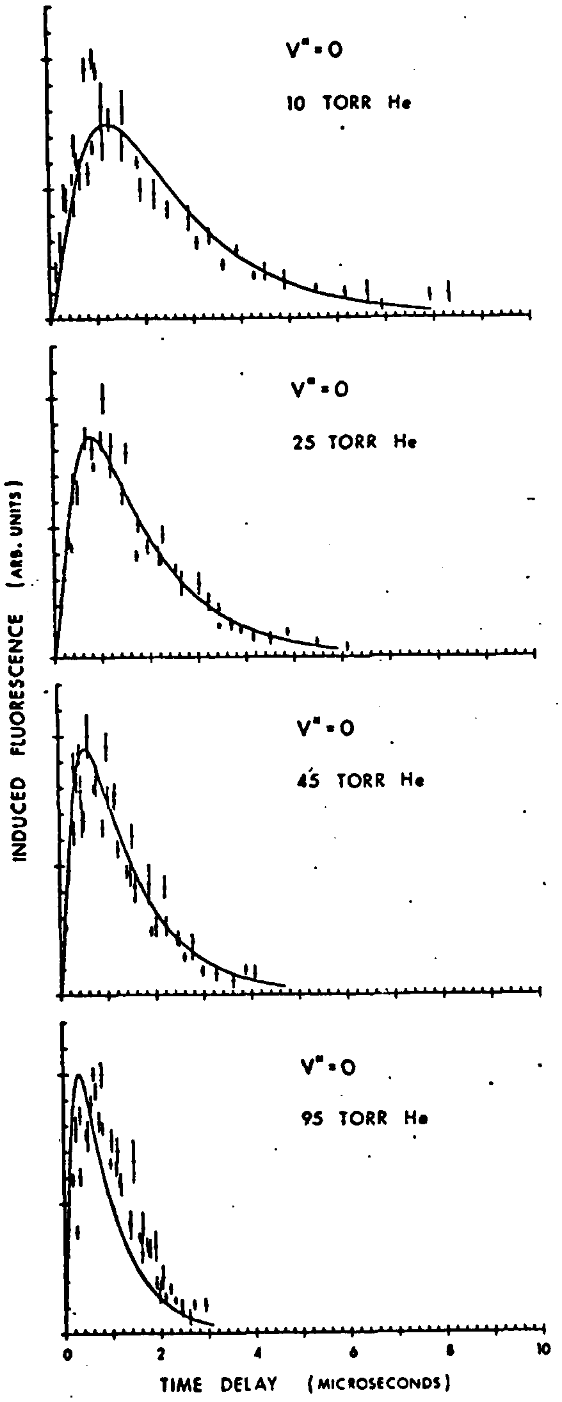
V" = 0
10 TORR He
V" = 0
25 TORR He
V" = 0
45 TORR He
V" = 0
95 TORR He
INDUCED FLUORESCENCE (ARB. UNITS)
0
2
4
6
8
10
TIME DELAY (MICROSECONDS)

Figure 2

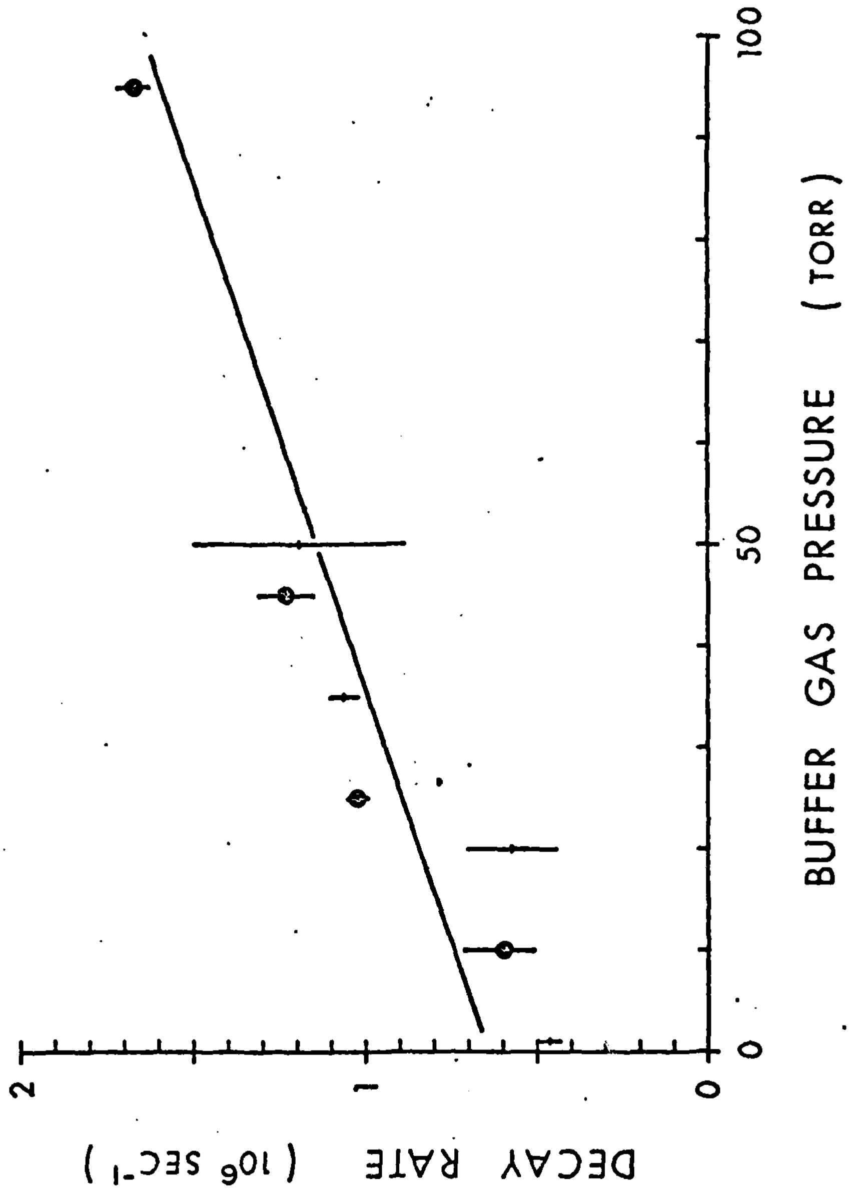

FIGURE 3

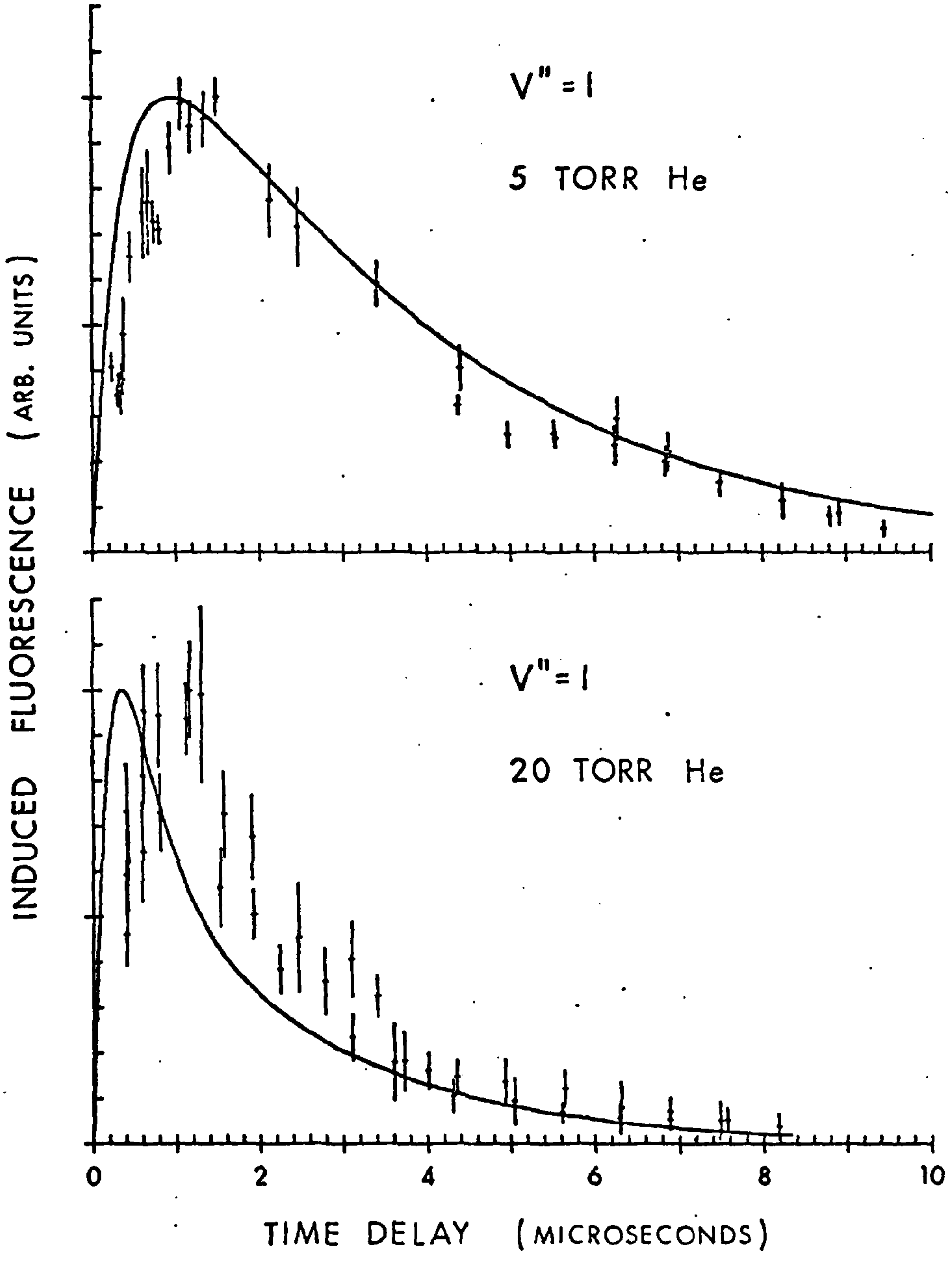
V" = 1
5 TORR He
V" = 1
20 TORR He
INDUCED FLUORESCENCE (ARB. UNITS)
0
2
4
6
8
10
TIME DELAY (MICROSECONDS)

FIGURE 4

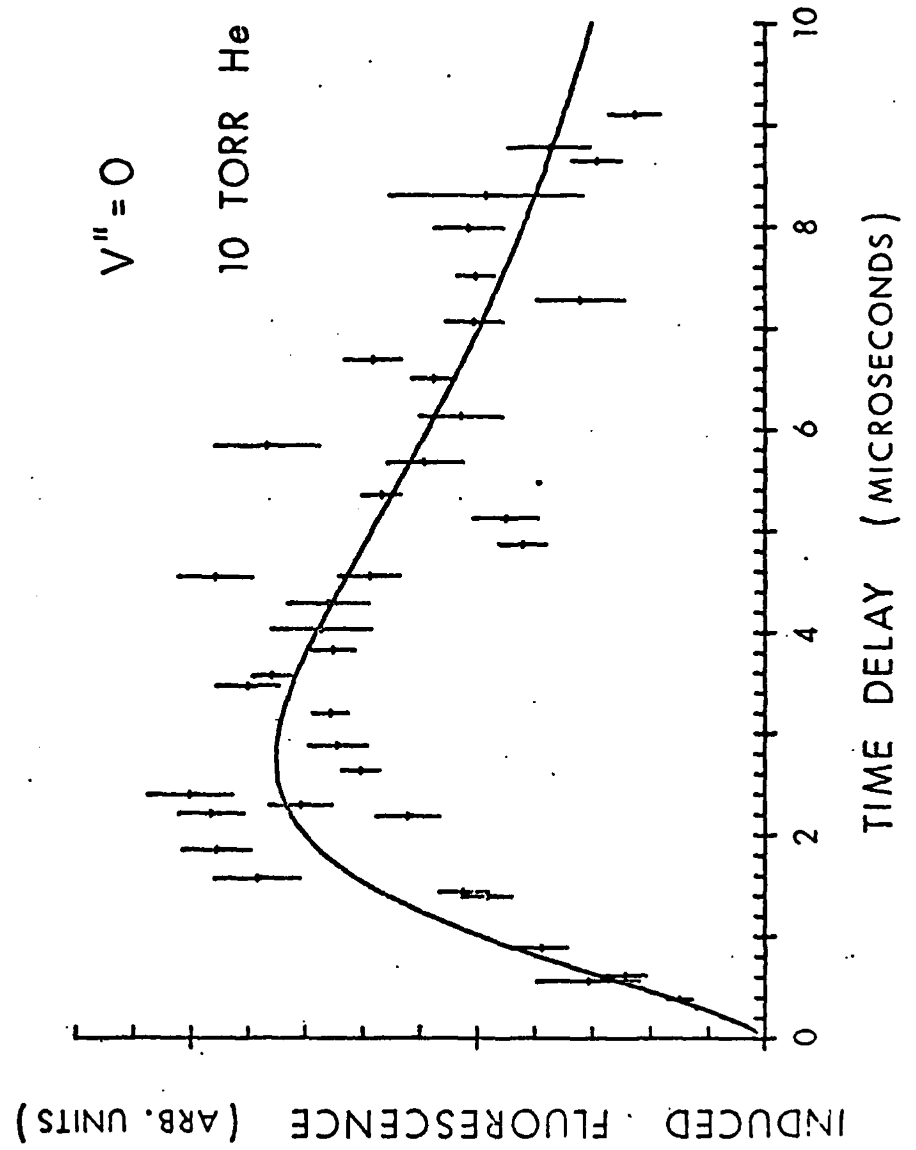
V" = 0
10 TORR He
0
2
4
6
8
10
TIME DELAY (MICROSECONDS)
INDUCED FLUORESCENCE (ARB. UNITS)

FIGURE 5

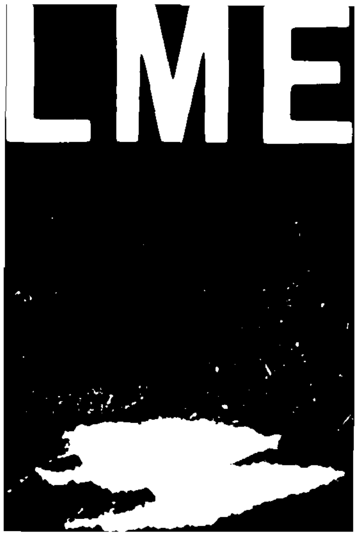
LME